Flux Lattice Melting, Flux Pinning, and Superfluid Density Tensor of $YBa_2Cu_3O_{7-\delta}$

R. Šášik and D. Stroud

Department of Physics, The Ohio State University, Columbus, Ohio 43210

(Received 29 November 1993)

We calculate the flux lattice melting curve $T_M(H)$ of $YBa_2Cu_3O_{7-\delta}$ for a magnetic field $\mathbf{H}\|\mathbf{c}$, in good agreement with experiment without any free parameters. We expand the Ginzburg-Landau order parameter in products of lowest Landau levels in the a-b plane and Bloch states in the c direction, evaluating the relevant statistical averages by Monte Carlo simulation. With no pinning, the c component of the superfluid density tensor jumps to a finite value at the transition, but the transverse components remain zero, corresponding to the sliding freedom of the flux lattice. With pinning present, the in-plane components become finite also. Relevant experiments are discussed.

PACS numbers: 74.60.Ec, 74.60.Ge, 74.76.Bz

In the high-T_c superconductors, with magnetic field $\mathbf{H}\|\mathbf{c}$, the Abrikosov lattice melts at a temperature $T_M(H)$ well below the upper, "mean-field" transition line $H_{c2}(T)$ [1]. Above $T_M(H)$ there is a finite density of Cooper pairs, but no long-range phase coherence, and a finite Ohmic resistivity [2]. The transition is believed to be highly sensitive to disorder, being either first order [3] or continuous [4] depending on the number and geometry of impurities. By contrast, the $H_{c2}(T)$ line is not a phase transition but rather a crossover temperature separating normal metal from melted flux liquid.

In this paper, we calculate the melting curve of the most thoroughly studied high-T_c material, $YBa_2Cu_3O_{7-\delta}$ (YBCO), without any free parameters. We characterize this melting curve by the *superfluid density tensor*. With no pinning, we find that the component of this tensor parallel to $\mathbf{H}$ becomes nonzero at the melting transition, but the components in the a-b plane remain zero. To produce nonzero a-b components as observed experimentally, we introduce a simplified pinning model which produces a harmonic restoring force on each vortex. This yields a superfluid density with a temperature dependence similar to experiment. Furthermore, by fitting the measured superfluid density to experiment at one field, we can in principle estimate the *strength* of this pinning potential.

In the absence of pinning, our approach has been described previously [5]. We start from a Ginzburg-Landau free energy functional with a *periodic*, *z-dependent* transition temperature with period d (z is the direction parallel to the c axis):

$$F=\int d^3\mathbf{r}\left\{\alpha(T-T_{c0}(z))|\psi(\mathbf{r})|^2+\frac{b}{2}|\psi(\mathbf{r})|^4+\frac{1}{2m^*}\left|\left(-i\hbar\nabla-\frac{e^*}{c}\mathbf{A}\right)\psi(\mathbf{r})\right|^2\right\}. \tag{1}$$

Here $T_{c0}(z)$ is the mean-field transition temperature of the material in zero field, $\mathbf{A}$ is the vector potential for the externally imposed magnetic field, $\psi(\mathbf{r})$ is the complex order parameter, α, b, and m^* are material-dependent constants, and c is the speed of light. The periodic z dependence of T_{c0} is introduced to characterize the underlying layered structure. The form (1) is appropriate when the penetration depth $\lambda_\perp$ for a field applied in the z direction is large compared to the mean vortex separation l_0. [We define $l_0=(4\pi/\sqrt{3})^{1/2}/\beta$, where $\beta^2=2eH/\hbar c$.] In practice, (1) is probably reasonable at sufficiently high fields, where $\lambda_\perp > (5\text{–}10)l_0$.

To calculate the thermodynamics, we expand $\psi(\mathbf{r})$ in basis functions $\Phi_{k_x,n}(\mathbf{r})=\phi_{k_x}(x,y)u(z-nd)$, where $\phi_{k_x}(x,y)$ is a state in the lowest Landau level in the x-y plane (the "LLL" approximation [6,7]), and $u(z-nd)$ is a (normalized) Wannier function for a state in the lowest Bloch band in the z direction. The corresponding Bloch eigenstate $\zeta_{k_z}(z)=\sum_{n=-\infty}^{\infty}e^{ik_znd}u(z-nd)$. As shown in [5], this choice of basis functions allows the *quadratic* part of the functional F to be diagonalized, since $T_{c0}(z)$ is assumed to be periodic in z. The LLL approximation is reasonable at high fields and near T_{c0}, since the higher Landau levels are separated from the first by a multiple of $\hbar\omega_c\equiv\hbar(2eH/m^*c)$, which increases with H. Similarly, for weakly coupled layers, it is reasonable to include only the lowest Bloch band in the nearest-neighbor tight-binding approximation, since the higher bands will be separated from it by a substantial energy gap.

With the gauge choice $\mathbf{A}=-Hy\hat{\mathbf{x}}$, the lowest Landau level is $\phi_{k_x}(x,y)=\exp(ik_xx)\varphi_0(y-k_x/\beta^2)$, where $\varphi_0(y)=(\beta^2/\pi)^{1/4}\exp(-\beta^2y^2/2)$. Expanding $\psi(\mathbf{r})=\sum_{k,n}c_{k,n}\times\Phi_{k,n}(\mathbf{r})$, we can express F as a sum of quadratic and quartic terms $F=F^{(2)}+F^{(4)}$, where

$$F^{(2)}=L_x\sum_{k,n}|c_{k,n}|^2(\tfrac{1}{2}\hbar\omega_c+E_0+\alpha T)-L_xt\sum_{k,n}c_{k,n}(c^*_{k,n+1}+c^*_{k,n-1}), \tag{2}$$

$$F^{(4)}=\frac{L_xb\beta}{\sqrt{8\pi}}u_{0000}\sum_{k,n}\sum_{q_1,q_2}c_{k,n}c^*_{k+q_1,n}c^*_{k+q_2,n}c_{k+q_1+q_2,n}\times V(q_1,q_2). \tag{3}$$

Here $V(q_1,q_2)=\exp[-(q_1^2+q_2^2)/2\beta^2]$ and u_{0000}

$=\int_{-\infty}^{\infty}|u(z)|^4 dz$. The sample is taken as a parallelopiped of dimension L_i in the ith direction.

The thermodynamics is determined by treating the complex coefficients $c_{k,n}$ as classical variables in the canonical ensemble. We have obtained correlation functions and other quantities for YBCO by Monte Carlo (MC) simulation, using the Metropolis algorithm, determining the parameters as in [5]. With the mass normalization $2e\hbar/m^*c=1$ they take the forms $\alpha=\frac{1}{2}|dH_{c2}/dT|_{T=T_{c0}(0)}$ and $t=\hbar c/4ged^2$, where $g\equiv m_\parallel/m^*$ is the effective mass ratio. The other parameters are $E_0=-\alpha\times T_{c0}(0)+2t$ and $b=2\pi\kappa^2$, where κ is the Ginzburg-Landau parameter. To estimate u_{0000} we assume that $T_{c0}(z)$ is sharply peaked at the twin CuO layers, which are separated by $d_0=3.2$ Å, and make the Kronig-Penney approximation $T_{c0}(z)=\tau_0+\tau\sum_{n=-\infty}^{\infty}[\delta(z-nd)+\delta(z-nd-d_0)]$. The lowest-energy Wannier function of this "potential" can easily be calculated in terms of τ, which is determined as in [5], by fitting the curvature at the bottom of the tight-binding band to the mass anisotropy g. This procedure yields the overlap integral t. The resulting $u_{0000}\approx 1/(8.3\text{ Å})$. The remaining numerical constants for YBCO are $T_{c0}(0)=93$ K, $|dH_{c2}/dT|_{T=T_{c0}(0)}=2\times10^4$ Oe K^{-1}, $d=11.4$ Å, $g=25$, and $\kappa\approx 100$.

Our Monte Carlo cell accommodates 64 flux lines and 28 layers in the z direction. Its dimensions are $L_x\times L_y\times L_z=8l_0\times 8(\sqrt{3}/2)l_0\times 28d\equiv V$. We have verified that the statistical averages are insensitive to L_z for $L_z>16d$. We use typically $\sim$1000 moves to thermally equilibrate the ensemble initialized in the ground state and the following $\sim$15000 moves to calculate running averages. A move is defined as one visit per coefficient $(c_{k,n})$.

To determine the melting curve of the "pure" (i.e., pin-free) YBCO, we consider the behavior of the helicity modulus (proportional to the superfluid density [8]) tensor

$$\gamma_{ij}=\left(\frac{\partial^2\mathcal{F}}{\partial A_i'\partial A_j'}\right)_{\mathbf{A}'=0}, \tag{4}$$

where $\mathcal{F}=-(k_BT/V)\ln\int\prod_{n,k}dc_{n,k}\,dc_{n,k}^*\exp(-F/k_BT)$ is the Helmholtz free energy per unit volume, and $\mathbf{A}'$ is an additional vector potential (beyond the one which produces $\mathbf{H}$) imposed in the presence of periodic boundary conditions. γ_{ij} measures stiffness against long-wavelength twists of the phases of ψ. In the defect-free crystal, γ_{ij} is diagonal with respect to the crystal axes coordinate system. We find that

$$\gamma_{zz}=2\left(\frac{2ed}{\hbar c}\right)^2 L_x t\left\langle\sum_{k,n}\mathcal{R}(c_{k,n}c_{k,n+1}^*)\right\rangle - 4\left(\frac{2ed}{\hbar c}\right)^2\frac{(L_xt)^2}{k_BT}\left\langle\left[\sum_{k,n}\mathcal{I}(c_{k,n}c_{k,n+1}^*)\right]^2\right\rangle, \tag{5}$$

while γ_{xx} and γ_{yy} are *identically zero*. ($\langle\cdots\rangle$ denotes a canonical average.) This seemingly counterintuitive result is due to the absence of intrinsic pinning in the defect-free crystal, which permits the Abrikosov lattice to slide freely in an applied phase twist.

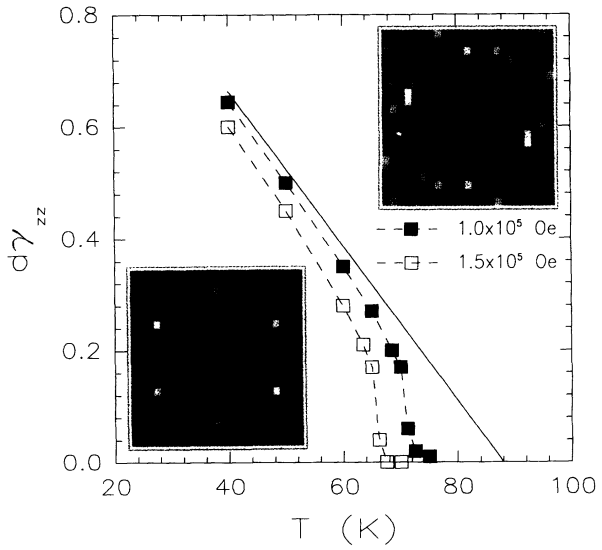

FIG. 1. Helicity modulus γ_{zz}, in Gaussian units, parallel to the field for "pure" (i.e., unpinned) YBCO at two different fields: $H=10^5$ Oe and $H=1.5\times10^5$ Oe, as obtained by Monte Carlo simulation. d is the period in the z direction. Dashed lines simply connect the calculated points. Full line: "mean field" γ_{zz}^{MF} at $H=10^5$ Oe. Numerical uncertainties are comparable to the symbol size or smaller. The insets show an intensity plot of the normalized structure factor $\tilde{\Gamma}^{(4)}(q_x,q_y,0)$, defined as in [5], at $H=1.5\times10^5$ Oe and temperatures $T=63.5$ and 67.5 K. Larger magnitudes of $\tilde{\Gamma}^{(4)}$ are indicated by greater brightness. The peaks at $\mathbf{q}=0$ have not been included in these plots.

Figure 1 shows $\gamma_{zz}(T)$ for YBCO at two different fields. γ_{zz} exhibits a rapid increase at the freezing temperature, consistent with (although certainly not proving) a first-order transition. Such a transition would best be demonstrated by searching for a double peak in the energy distribution function at the transition temperature, as has been found in the *two-dimensional* version of this model in a planar geometry, using a Landau gauge [9,10]. A transition was also obtained for the two-dimensional model using a symmetric gauge [6], although no transition was found with a symmetric gauge on a sphere [11]. A first-order transition has been also found in a frustrated XY model on a stacked triangular lattice [12], which can be viewed as a simplified model for the three-dimensional melting studied here. The solid line represents the "mean-field" value of γ_{zz}. This is obtained by evaluating (5) in the ordered ground state, with nonzero coefficients $c_{(2m)q_0,n}^{MF}\equiv c_0=[\alpha(T_c(H)-T)/\beta bu_{0000}]^{1/2}/(\sqrt{3}\pi/\beta_A^2)^{1/4}$, $c_{(2m+1)q_0,n}^{MF}=ic_0$, where m is an integer, $\beta_A=1.159595\ldots$ is the Abrikosov ratio, and $q_0=2\pi/l_0$. The corresponding helicity modulus is $\gamma_{zz}^{MF}=(4d/\sqrt{3}l_0)\times(2e/\hbar_c)^2tc_0^2$.

During our MC simulations, we also monitored the density-density correlation function in the x-y plane, its Fourier transform $\tilde{\Gamma}^{(4)}(q_x,q_y,0)$, and the two-point corre-

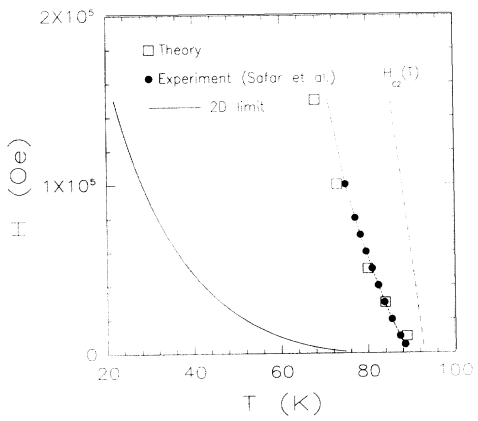

FIG. 2. Flux lattice melting curves for unpinned YBCO. Open squares: calculated points, as obtained from MC simulation. Full circles, connected by a dotted line: experiment [13,14]. Dashed curve: upper critical field $H_{c2}(T)$. Lower full curve: calculated melting curve in the "two-dimensional limit" [10], from Hamiltonian (2) and (3) with $t=0$.

lation function $\Gamma^{(2)}(0,0,z)$, all defined as in [5], in various individual configurations. In Fig. 1, we show a snapshot of $\tilde{\Gamma}^{(4)}(q_x,q_y,0)$ in a particular equilibrated configuration at $H=1.5\times10^5$ Oe and temperatures $T=63.5$ and 67.5 K, just below and above melting. Clearly, the Bragg peaks disappear and an isotropic liquid phase sets in at the *same* temperature where γ_{zz} goes to zero. Likewise, we find that long-range order in $\Gamma^{(2)}(0,0,z)$ disappears above this melting temperature. Thus, melting occurs here at the same temperature in the x-y plane and the z direction.

The melting curve deduced from the vanishing of γ_{zz} is shown in Fig. 2, where it is compared to experiment [13,14] in a twin-free single crystal of YBCO. Agreement with experiment is remarkably good over a broad range of fields from about 10^4 to 1.5×10^5 Oe, even though the theory is expected to be best only at the higher fields [15]. For comparison, we also show the predicted 2D melting curve [10], obtained from this model in the limit $t\to 0$.

Pinning can be introduced into the present model by allowing the parameters in (1) to be position dependent. As a highly simplified illustration, we introduce a commensurate pinning potential which produces a harmonic restoring force on any vortex displaced from its mean-field equilibrium position, as assumed, e.g., by [16]. Obviously, such a potential leaves out many realistic features, notably the expected disorder, but it does provide a soluble model. To generate such a potential, we make the replacement

$$T_{c0}(z)\to T_{c0}(\mathbf{r}_\perp,z)=T_{c0}(z)-\mu_p T_{c0}(0)\sum_{\mathbf{R}_i}\delta(\mathbf{r}_\perp-\mathbf{R}_i)\,, \tag{6}$$

where $\mathbf{R}_i$ denotes the (two-dimensional) position of a

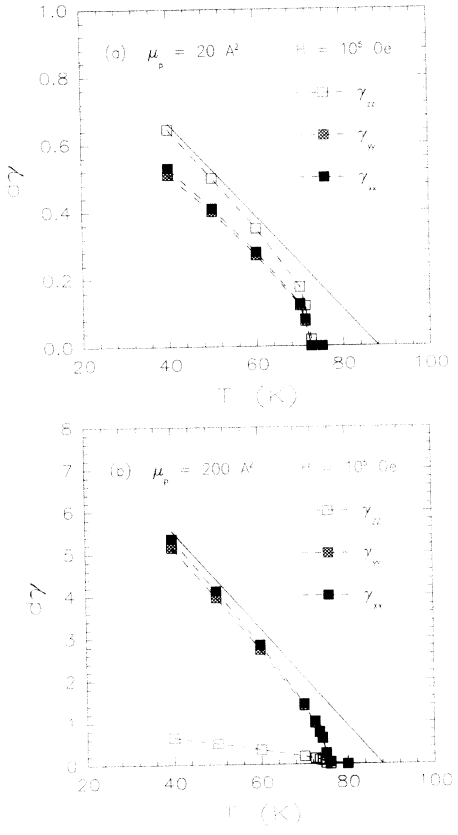

FIG. 3. Helicity moduli γ_{xx}, γ_{yy}, and γ_{zz}, in Gaussian units, for "pinned" YBCO at $H=10^5$ Oe and two different pinning strengths: (a) $\mu_p=20$ Å^2; (b) $\mu_p=200$ Å^2. The dashed lines simply connect the calculated points. Full curves: mean-field values of γ_{zz} (a) and γ_{xx} (b). Cases (a) and (b) correspond to a local depression of T_{c0} by 1% and 10% in a pinning center of diameter 50 Å.

point in a triangular lattice commensurate with the lattice of flux lines, $\mathbf{r}_\perp\equiv(x,y)$, and μ_p is the strength of the commensurate pinning potential. The ground state of this system can still be conveniently expanded in LLL's near the H_{c2} line.

Figure 3 shows γ_{xx}, γ_{yy}, and γ_{zz} at a field of 10^5 Oe for two different pinning strengths μ_p. Evidently, for this form of pinning, even the weaker pinning potential is sufficient to cause γ_{xx} or $\gamma_{yy}\approx\gamma_{zz}$. (This is weak pinning, since the smaller μ_p would correspond to a depression of T_{c0} by 1% over 10% of the sample area. By comparison, a typical "strong" pinning center might represent a local depression of T_{c0} to *zero* over such an area.) Since numerically $\gamma_{xx}\approx\gamma_{yy}$, we will denote both by $\gamma_\perp$. The temperature dependences of all three moduli are similar, following the expected linear behavior of $\langle|\psi|^2\rangle$ (where the bar denotes a spatial average), but dropping simultaneously to zero at an apparently *single* melting temperature [17]. This single transition we obtain seems reasonable in our model, however weak the interlayer coupling, because as soon as $\gamma_{zz}>0$, the thickness of the

film in the z direction is effectively infinite, driving the "two-dimensional" transverse ordering transition up to the same temperature.

The helicity modulus tensor can be measured directly, e.g., by studying the inductive response of a superconducting film. To make this connection, note that the *first* derivative of the free energy is the local current density $\mathbf{J}$, i.e., $(\partial \mathcal{F}/\partial A_i')_{\mathbf{A}'=0} = -J_i/c$. Hence, $\gamma_{ij} = -c^{-1}(\partial J_i/\partial A_j')_{\mathbf{A}'=0}$. If $\mathbf{A}'$ is produced by an ac electric field $\mathbf{E}$ of frequency ω, then $\mathbf{A}' = -ic\mathbf{E}/\omega$. This gives $\gamma_{ij} = -i\omega \times \sigma_{ij}/c^2$, where $\sigma_{ij} \equiv (\partial J_i/\partial E_j)_{\mathbf{E}=0}$ is the (purely imaginary) conductivity of the sample at very low frequencies. In recent measurements on (effectively two-dimensional) a-MoGe films with moderate to weak pinning [18], a sharp drop in the imaginary part of the film admittance was observed, in qualitative agreement with the behavior of $\gamma_\perp$ in Fig. 3 [19].

We can use (6) to estimate the so-called Labusch parameter [16,20] α_L (the "spring constant") acting on a given vortex when it is displaced from its equilibrium position. Assuming that the vortex lattice is in its ground state configuration for a given temperature, α_L will be given by the second derivative of F with respect to displacement, evaluated at the position of the local energy minimum. The result is (in Gaussian units) $\alpha_L \approx 1.58\mu_p \times T_{c0}(0)\{[T_c(H) - T]/bu_{00000}\}2eH/\hbar c$. This represents the spring constant per double CuO layer when a vortex line is displaced from equilibrium.

There is some possible experimental evidence for a single flux lattice melting transition in an unpinned layered superconductor, characterized by a nonzero γ_{zz} but zero $\gamma_\perp$. This comes from measurements on an artificially prepared layered MoGe/Ge heterostructure [21]. In this material, the melting transition was characterized by a sharp drop in the dc resistivity *perpendicular* to the layers, but not the component parallel to the layers. This behavior was interpreted as the onset of rigidity in vortex lines perpendicular to the layers which were, however, disordered in the x-y plane. The present results, however, suggest another possibility, namely, that a *three-dimensional* vortex lattice forms at the transition temperature, but remains free to move perpendicular to the magnetic field, producing flux-flow resistivity. This behavior might be plausible if the in-plane pinning is sufficiently weak. In YBCO, the three-dimensional transition which we calculate is characterized by a sharp drop in *in-plane* resistivity [13]. This suggests some point disorder, strong enough to produce pinning of the 3D lattice, but not sufficient to destroy the first-order transition, at least at moderate fields. Apparently such pinning always exists in YBCO because of unavoidable randomness due to oxygen vacancies or interstitials. Figure 3 suggests that arbitrarily weak commensurate pinning produces a zero-resistance state.

We thank S. M. Girvin, T. R. Lemberger, A. H. MacDonald, M. A. Moore, Z. Tešanović, and L. Wagner for valuable conversations. This work has been supported by NSF, through Grant No. DMR90-20994, and by the Midwest Superconductivity Consortium, through DOE Grant No. DE-FG-02-90-ER45427. Calculations were carried out, in part, on the CRAY Y-MP 8/8-64 of the Ohio Supercomputer Center.

[1] D. R. Nelson, Phys. Rev. Lett. **60**, 1973 (1988); D. R. Nelson and S. Seung, Phys. Rev. B **39**, 9153 (1989); A. Houghton, R. A. Pelcovits, and A. Sudbø, Phys. Rev. B **40**, 6763 (1989); S. Ryu *et al.*, Phys. Rev. Lett. **68**, 710 (1992); P. L. Gammel *et al.*, Phys. Rev. Lett. **61**, 1666 (1988); D. E. Farrell, J. P. Rice, and D. M. Ginsberg, Phys. Rev. Lett. **67**, 1165 (1991).

[2] M. C. Marchetti and D. R. Nelson, Physica (Amsterdam) **174C**, 40 (1991).

[3] E. Brézin, D. R. Nelson, and A. Thiaville, Phys. Rev. B **31**, 7124 (1985).

[4] D. S. Fisher, M. P. A. Fisher, and D. A. Huse, Phys. Rev. B **43**, 130 (1991).

[5] R. Šášik and D. Stroud, Phys. Rev. B **48**, 9938 (1993).

[6] Z. Tešanović and L. Xing, Phys. Rev. Lett. **67**, 2729 (1991); Z. Tešanović, Phys. Rev. B **44**, 12635 (1991).

[7] G. J. Ruggeri and D. Thouless, J. Phys. F **6**, 2063 (1976).

[8] The connection between superfluid density and helicity modulus was first made, for isotropic superfluids, by M. E. Fisher, M. N. Barber, and D. Jasnow, Phys. Rev. A **8**, 1111 (1973). Note that the superfluid density is not, in general, identical to the local density of Cooper pairs.

[9] Y. Kato and N. Nagaosa, Phys. Rev. B **48**, 7383 (1993).

[10] J. Hu and A. H. MacDonald, Phys. Rev. Lett. **71**, 432 (1993).

[11] J. A. O'Neill and M. A. Moore, Phys. Rev. B **48**, 374 (1993).

[12] R. Hetzel, A. Sudbø, and D. A. Huse, Phys. Rev. Lett. **69**, 518 (1992).

[13] H. Safar *et al.*, Phys. Rev. Lett. **70**, 3800 (1993).

[14] The "experimental" line of Fig. 2 is the line of first-order transitions of Ref. [13] which changes, at 10^5 Oe, to a line of second-order transitions (not shown).

[15] Although we have carried ours to fields lower than $H_{c2}(T)/3$, arguments due to Z. Tešanović (private communication) suggest that the LLL approximation may actually break down only when the *sixth* LL is activated, i.e., for $H < [1/(2\times 6+1)]H_{c2}(T)$.

[16] J. R. Clem and M. W. Coffey, Phys. Rev. B **46**, 14662 (1992).

[17] A *double* transition has been observed in a uniformly frustrated XY model on a cubic lattice with frustration $f = \frac{1}{25}$ but not at $f = \frac{1}{5}$. [Y.-H. Li and S. Teitel, Phys. Rev. B **47**, 359 (1993); **45**, 5718 (1992).]

[18] A. Yazdani *et al.*, Phys. Rev. Lett. **70**, 505 (1993).

[19] D. S. Reed *et al.*, Phys. Rev. B **47**, 6150 (1993), have reported scaling measurements of the complex conductance in twinned crystals. D. Xenikos and T. Lemberger (private communication) have measured a $\gamma_\perp$ of an YBCO film which has a linear temperature dependence and a sharp drop similar to Fig. 3.

[20] A. M. Campbell and J. E. Evetts, *Critical Currents in Superconductors* (Barnes & Noble, New York, 1972).

[21] D. G. Steel, W. R. White, and J. M. Graybeal, Phys. Rev. Lett. **71**, 161 (1993).

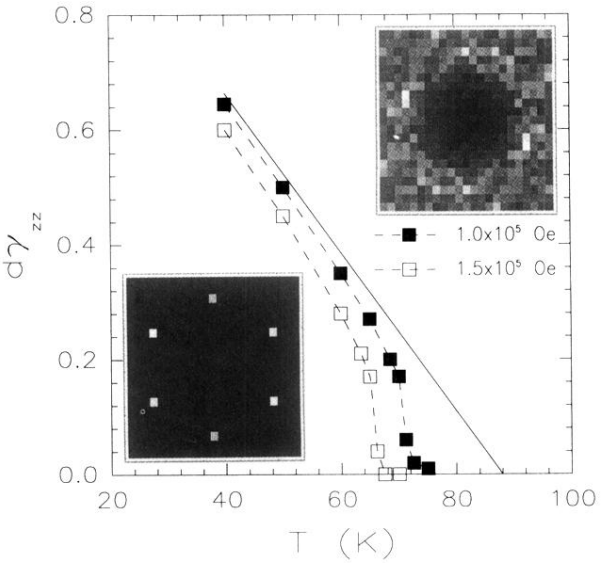

FIG. 1. Helicity modulus γ_{zz}, in Gaussian units, parallel to the field for "pure" (i.e., unpinned) YBCO at two different fields: $H=10^5$ Oe and $H=1.5\times10^5$ Oe, as obtained by Monte Carlo simulation. d is the period in the z direction. Dashed lines simply connect the calculated points. Full line: "mean field" γ_{zz}^{MF} at $H=10^5$ Oe. Numerical uncertainties are comparable to the symbol size or smaller. The insets show an intensity plot of the normalized structure factor $\tilde{\Gamma}^{(4)}(q_x,q_y,0)$, defined as in [5], at $H=1.5\times10^5$ Oe and temperatures $T=63.5$ and 67.5 K. Larger magnitudes of $\tilde{\Gamma}^{(4)}$ are indicated by greater brightness. The peaks at $\mathbf{q}=0$ have not been included in these plots.